Eur Biophys J (2011) 40:1081–1085
DOI 10.1007/s00249-011-0725-0

ORIGINAL PAPER

Real-time detection of changes in the electrophoretic mobility of a single cell induced by hyperosmotic stress

Pau Mestres · Dmitri Petrov

Received: 17 March 2011 / Revised: 8 June 2011 / Accepted: 12 June 2011 / Published online: 28 June 2011

Abstract Living cells survive environmentally stressful conditions by initiating a stress response. We monitored changes in the electrophoretic mobility (EPM) of single, optically trapped yeast cells under hyperosmotic stress conditions using optical tweezers combined with a position detector. We studied the dynamics of the EPM stress response for cells at different phases of the cell cycle.

Keywords Living cell · Electrophoretic mobility · Hyperosmotic stress · Optical tweezers

Introduction

The cell stress response is the reaction of a living cell to ambient changes that are potentially harmful, for example, an increase in temperature, pH, or saline concentration, or the presence of toxins. In some instances, stress responses may eventually lead to stress tolerance as a long-term defense mechanism against cytotoxic agents (Storey and Storey 2002; Hohmann and Mager 2002). The response of living cells to external stresses may be detected using fluorescent tags (Wadskog et al. 2006; Eriksson et al. 2007), microfluidic engineering methods (Lee et al. 2008; Rowata et al. 2009), and Raman spectroscopy (Singh et al. 2005; Eriksson et al. 2007). In particular, combining Raman spectroscopy with the optical tweezers technique (Petrov 2007; Chan et al. 2008), it was shown that, when glucose was used to exert hyperosmotic stress in a *Saccharomyces cerevisiae* yeast cell, two chemical substances—glycerol and ethanol—can be monitored in real time in the single cell (Singh et al. 2005).

Cellular electricity plays an important role throughout the whole cell cycle. As phosphate compounds, amino acids, or ions are carried through the cell membrane, their movement sets up an electrical current, which creates a voltage differential across the cell membrane. Living cells may also have spatially localized charged groups. When placed in an electric field, the cell moves as a whole, resulting in cell electrophoretic mobility (EPM).

Nonmonotonic behavior of EPM during the cell cycle was recently observed: the maximum EPM occurred at the initial stage of growth, strongly reducing when the cell cycle was near its final stage (Tonin et al. 2010). During cell growth, changes in the EPM may occur due to continuous redistribution of cell organelles and size changes.

In this report we consider a perspective different from our previous Raman study of the hyperosmotic stress response of living cells (Singh et al. 2005). Here, we monitor how the EPM changes when a single living cell at different stages of its life cycle is subjected to hyperosmotic stress.

Experimental section

We chose the *Saccharomyces cerevisiae* yeast cell as the object of study. This is an excellent model organism for research in cellular and molecular biology. Since the basic general biochemical mechanisms are highly conserved

P. Mestres · D. Petrov (✉)
ICFO—The Institute of Photonic Sciences,
Av. Carl Friedrich Gauss, num. 3, 08860 Barcelona,
Castelldefels, Spain
e-mail: Dmitri.Petrov@icfo.es

D. Petrov
ICREA—Institucio Catalana de Recerca i Estudis Avancats,
Barcelona, Spain

among all eukaryotes, most current understanding of cell cycle processes such as replication, transcription, translation, and protein sorting originally came from experiments performed on yeast (Cooper 2000). The majority of genes in yeast are homologous to those in humans; hence, molecular biological tools involving yeast are indispensable for advancement in fields such as anticancer research (Bassett et al. 1996). Besides being used in the baking industry, yeasts are also important for production of industrial chemicals and fuels (Stanbury et al. 1984).

The cell cycle of an individual yeast cell can be divided into four phases: mitosis, G1 (gap), synthesis, and G2 (gap). Nuclear division occurs during mitosis. The period after this but before the initiation of nuclear DNA replication, during which the cell monitors its environment and its own size, is known as the G1 phase. DNA synthesis occurs during the synthesis phase. The period between the completion of nuclear DNA replication and mitosis is termed the G2 phase. The cell cycle of the cell is regulated primarily at a point in late G1 when a bud forms and continues growing until it separates from the mother cell after mitosis. Morphological changes occur as the cell enters the cell cycle. This can be detected under a microscope.

In our experiments, cells were grown in yeast extract–peptone–glucose (YPD broth; Sigma Aldrich) medium with complete supplement under standard conditions. In all measurements, cells were placed in a homemade microfluidic chamber with electrodes, and diluted further in YPD such that a single cell could be trapped with no other cells in the surrounding medium. The pH of the medium was 6.5 to ensure cell viability throughout the growing process.

Previously, an experimental platform where optical tweezers and epifluorescence microscopy are combined with a microfluidic system to enable analysis of rapid cytological responses in single cells, including *Saccharomyces cerevisiae* yeast cells, was suggested and explored (Eriksson et al. 2007a, b, 2010). In our experiments, two new elements were used: electrodes to provide an electrical field, and a position detection system to obtain information on the motion of the cell. A 985-nm optical beam from a laser coupled to a single-mode fiber (3S Photonics, 1999CHP pump module), expanded up to 8 mm and then focused by a 100×, NA = 1.3 microscope objective (Nikon, CFI PL FL 100×), was used for cell trapping (Fig. 1).

The trapping beam size was approximately 1 μm in diameter, and the size of the cell was about 5 μm. An additional 635-nm optical beam from a low-noise laser (Coherent, ultralow-noise diode laser LabLaser635) coaxial with the trapping beam was used for cell position detection, using the back focal-plane interference between the light diffracted by the optically trapped cell organelles and the undiffracted beam (Gittes and Schmidt 1998). The forward scattered light of the detection beam was collected by a

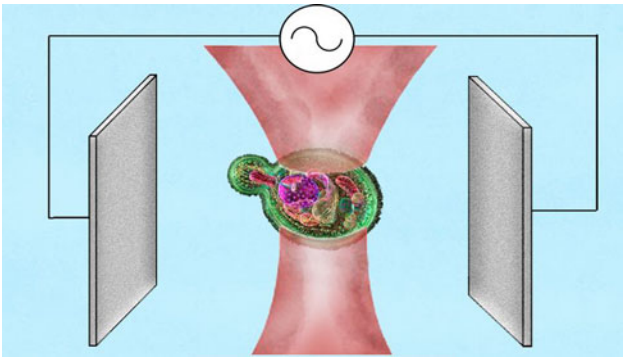

Fig. 1 An optically trapped single cell in an AC electrical field

40× objective and analyzed by a position detector (Newport, 2931 position-sensitive detector). The forward scattered light of the trapping beam was blocked by a short-pass filter (Thorlabs FES0700). The resulting signals were then transferred through an analog-to-digital conversion card (National Instruments PCI-6120) to computer software.

From our previous experiments (Singh et al. 2005, 2006) the optical power at the sample should be less than several milliwatts to permit the cell to grow even in the optical trap. In our experiments with trapping power of approximately 1 mW and without an external electric field, the cell grows following its normal cell cycle. Also, at such low optical trapping power, we did not observe cell orientation along the optical axis of the trapping beam when a bud appears. The power of the detection beam was smaller than the trapping power, and the detection beam alone could not trap the cells.

The position detection system did not allow measurement of absolute values of cell movement. In fact, all known methods to find a relation between the position detector signal and real position, such as the drag force method or fitting of the power spectrum density function of the Brownian motion of an optically trapped object [see, for example, Lee et al. (2007)], require knowledge of the size of the trapped particle (assumed to be a sphere) and the viscosity of the surrounding medium. In our experiments, high-refractive-index granules of different sizes embedded in the cytoskeleton are trapped by the focused optical beam, and the cell as a whole is immobilized near the beam focus (Tolic-Norrelykke et al. 2004). Neither the size of these specific parts of the cell nor the viscosity of the surrounding fluid is known with high accuracy. Moreover, scattering of the detection beam by the optically trapped cell at different stages of its cell cycle may vary due to changes of the size of the trapped part. We found, however, that the total intensity of the scattered detection beam did not change considerably during cell growth. Therefore, although calibration of the optical trap was not possible, the amplitude of the

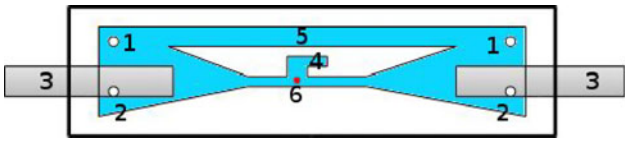

Fig. 2 Channels for liquid are shown in *blue*. The holes labeled 1 were used as input and output for injection of growth medium with cells. The holes labeled 2 were used as input and output for injection of glucose solution. Electrodes are labeled 3. A channel (labeled 5) was added to divide the input flux and reduce it at the trapping point 6. We added a narrow channel 4 without output where we kept the optically trapped cell while injecting the glucose solution

cell motion presented in the figures in arbitrary units is proportional to the output signals from the position detector, and characterizes the movement of the optically trapped organelles and, hence, the EPM response.

We exerted hyperosmotic stress on the optically trapped cell at a given stage of its cell cycle by injecting 100 mg/ml glucose solution into the growth medium in the fluid chamber. The flux of the solution did not remove the cell under study from the optical trap, since we used the special geometry of channels shown in Fig. 2.

The parameters of the electric field applied to the optically trapped cell were chosen according to the following observations: the electric field has to be minimal in order to reduce the possibility of relative motion of the charged parts (thereby preventing disturbance of the growth process). Hence, an AC signal is preferable. We used a 20 V AC voltage at frequency of 1 Hz, which corresponds to an electric field of approximately 1,500 V/m near the trapping beam focus for the geometry of fluid chamber channels and electrodes used. With this value, we could measure the AC component of the position signal at different stages of cell growth. A limiting factor here is the Brownian motion of the trapped cell, which induces unavoidable noise in the position detection output signal.

We noticed, however, that cell growth was impossible even when a minimal AC electric field was applied continuously during several tens of minutes. A separate study is needed to explain this experimental finding from a biochemical point of view.

We overcame this difficulty using the following protocol. A single yeast cell at the beginning of the cell cycle was trapped and allowed to grow to a given phase of its life cycle. The cell's growth was monitored by acquiring microscopic images and observing morphological changes. When the optically trapped cell reached the desired stage, the electric field was switched on for 25 s, and the position detector signal was acquired at a rate of 2 kHz. This gave us information on the initial value of the EPM before hyperosmotic stressing. After acquiring the data, the electric field was switched off, and the cell was displaced to position 4 of the fluid chamber (Fig. 2) by moving the flux chamber with

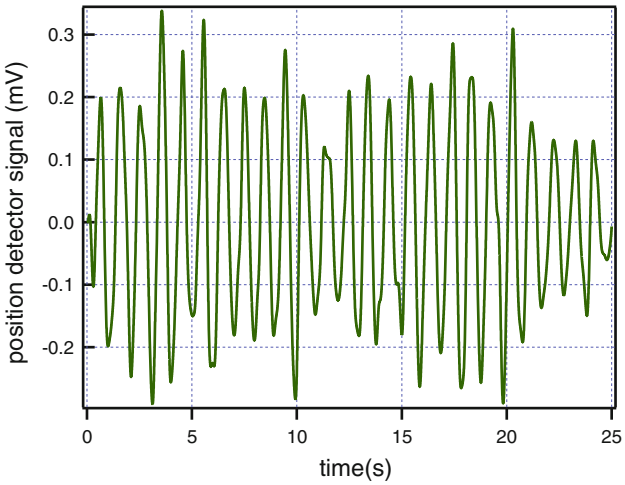

Fig. 3 Filtered signals of the position detector

computer-controllable screws. The glucose solution was injected simultaneously through the pair of inputs 2, and after 2 min the cell was displaced back to the initial position 6. The entire procedure required about 15 min. Next, the electrical field was switched on for 25 s, followed by data acquisition, after which the cell was allowed to grow for 10 min in the presence of the hyperosmotic stress but without the electric field. Then, for 25 s, the EPM measurements were performed again. This protocol provided information on the time dependence of the EPM hyperosmotic stress response.

Figure 3 shows example experimental data obtained from the position detector during 25 s, passed through a Butterworth filter, which permits reduction of high-frequency (above 5 Hz) components in the output signal due to Brownian motion. As seen, the position signal is periodic; however, the oscillation amplitude changes by up to 20% during the acquisition period. The variations of the amplitude are quite regular, which permits one to suppose the presence of two frequencies in the output signal. The low-frequency component is due to rotational motion of the cell (as observed also visually). In fact, the optical beam traps parts of the cell with high refractive index, which may not coincide spatially with electrically charged parts of the cell. Therefore, the charged parts of the cell moving linearly in the electric field are displaced relative to the optically trapped area of the cell, causing cell rotation. The experimental points and error bars shown on the figures indicate average values of the oscillation amplitude at 1 Hz frequency and the standard deviation during a period of 25 s.

We studied the EPM stress response of the cells in three phases of growth (late G2, early budding, and advanced budding phase). We started each experiment by trapping a new-born daughter cell. The cell then grew without the

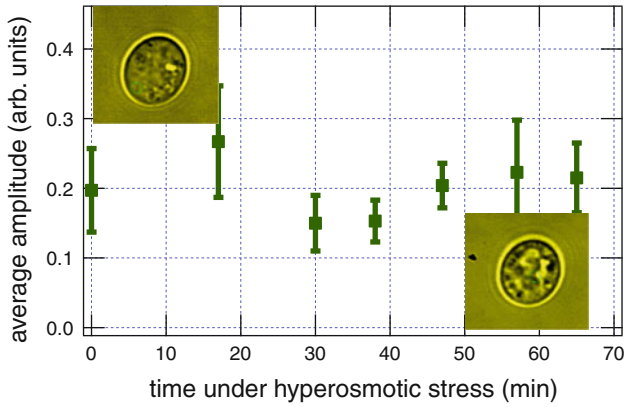

Fig. 4 EPM time dependence for the cell under hyperosmotic stress when the initial state was the late G2 phase. *Insets* show microscope images at the beginning and end of the experiment

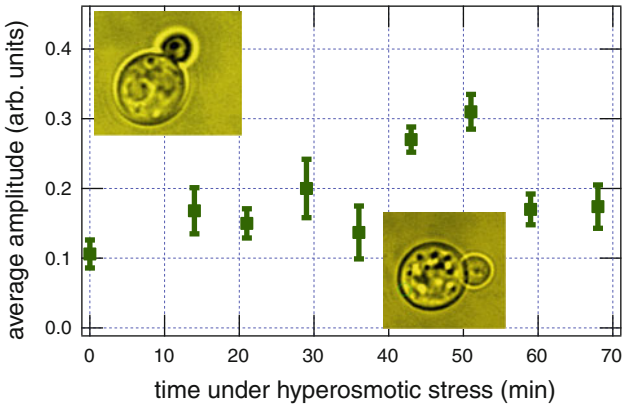

Fig. 5 EPM time dependence of the cell under hyperosmotic stress when the initial state was the early budding phase. The size of the bud was less than one-quarter of the mother cell size. *Insets* show microscope images at the beginning and end of the experiment

electric field applied to the electrodes. We continuously observed the cell's morphological changes, i.e., its shape and appearance. We started the above-described protocol for the EPM measurements in the presence of the hyperosmotic stress only for cells that: (1) reached a specific size as measured by a calibrated microscopic system, (2) had a similar appearance, and (3) for which the trapping point was at a similar distance from the cell membrane. Not all cells selected by these parameters could be trapped during 60 min (we chose this time as it is comparable to the whole cell cycle duration), as some of them escaped from the trap due to the extremely low trapping power.

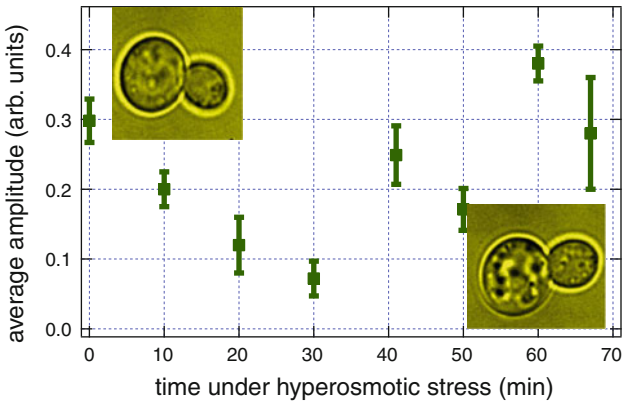

Fig. 6 EPM time dependence of the cell under hyperosmotic stress when the initial state was the advanced budding phase. The size of the bud was more than one-half of the mother cell size. *Insets* show microscope images at the beginning and end of the experiment

Results

Experiments were done with about 20 cells, each of which was preliminary selected from the cells injected into the fluid chamber according to the above-described protocol. All experimental data showed that the effect of the hyperosmotic stress was so fast and strong that it practically stopped the time dependence of the EPM compared with our previous measurements of the EPM of a growing cell under normal conditions (Tonin et al. 2010). Therefore, since practically no quantitative time dependence of the EPM might be detected, in this report we restrict our analysis to only demonstrating the typical time behavior of EPM for cells at different phases of growth (Figs. 4, 5, 6). There were three cells for each stage that could be trapped during 60 min.

First, we give a summary of morphological observations. (1) Cell growth stopped (or slowed down) regardless of the cell phase at which the hyperosmotic experiment began. (2) After adding the glucose, shrinkage of the cell was observed together with morphological changes causing an increase of the contrast of organelles's images in the cell (see insets in the following figures). (3) After changing the medium that exerted the hyperosmotic stress to the growth medium, growth of the cell resumed.

Measurements of the EPM time dependence under the stress condition showed that, for cells subjected to stress at the late G2 phase or early budding phase, the EPM remained constant. For cells subjected to stress at the advanced budding phase, slight increase of EPM for approximately 30–40 min after the application of the stress conditions was observed for all three cells. Since the cells were preliminarily selected to have the same morphological parameters before the hyperosmotic stress was applied, this tendency may be considered as probably due to the fact that the EPM of all three cells studied behaved similarly, bearing in mind also that several other cells that we could trap during 10–30 min gave the same result.

Discussion

Previously we showed that, in growth medium, the EPM increases about threefold relative to its initial value during the first 20 min (Tonin et al. 2010). Thereafter, the EPM decreases and, by the end of the cell cycle, falls back to the value measured at the beginning of the cycle. EPM increase in the mitotic phase is due to division of the chromosomes in the cell nucleus, cytoplasm, organelles, and cell membrane into two cells. The EPM decreases after 50 min, when the cell is in the synthesis phase and nuclei formation in the bud has completed. Hence, the cell exhibits strong EPM only during a relatively short period of the mitotic phase of the whole cell cycle. The EPM of the cell in other phases is much lower than in the mitotic phase, even though the volume of the cell continues to increase and the cell component spatial redistribution processes are still active.

Bearing in mind our previous observations of EPM dynamics for yeast cells growing under normal conditions, we suggest the following interpretation of the EPM hyperosmotic stress response.

When the cell membrane is subjected to hyperosmotic stress conditions, a stress response mechanism is triggered. This evokes intracellular changes, such as temporal arrest of the cell cycle, membrane depolarization (Delleya and Halla 1999), and a contribution of water from vacuoles to the cytoplasm due to its leakage through the membrane under hyperosmotic conditions. This loss of water explains why the organelles could be observed with greater contrast after a few minutes in the hyperosmotic medium. It is also possible for the cell to undergo some internal repairs or cytoskeleton modifications, if some internal damage has been caused by the osmotic pressure. These processes can significantly modify the dipole moment of the cell and lead to random reorientations of the cell as a dipole, resulting in periods of a chaotic oscillation behavior interleaved with periods where the oscillations correlate perfectly with the electric field.

One of the most important mechanisms known to occur in yeast cells to counter hyperosmotic stress is production of glycerol, which acts as a protector against osmosis, reequilibrating the osmotic pressure (Hohmann and Mager 2002). It was reported that an increase of the intracellular glycerol concentration occurs in approximately 40 min after the stress begins (Singh et al. 2005). Based on this observation, we may relate the EPM increase for cells subjected to the stress at the advanced budding phase to this glycerol production mechanism. However, although the cell undergoes numerous internal changes in order to be able to resume the normal cell cycle, the osmotic pressure is still too high to allow the cell to continue its growth. This is proved by the fact that, if we remove the hyperosmotic medium, the cell growth resumes.

Many details of the EPM stress response remain unclear. The main conclusion of this study is that the effect of hyperosmotic stress is so strong that it practically stops any temporal dependence of the EPM. Future work will involve consideration of all parameters, probably combined with potentiometric probes, or charge/potential-sensitive fluorescent probes (Eriksson et al. 2007a; Lakowicz 1999). However, the results presented herein demonstrate an additional tool for examining the mechanisms of single living cell responses to alteration of environmental conditions, offering an alternative measure to standard biophysical assays. The experimental setup is also suitable for lab-on-a-chip applications.

Acknowledgments We thank M. Tonin for fruitful discussions, S. Balint for his help in preparation of cells and medium, V. Petrov for his help in manuscript preparation, and Fundació Privada Cellex Barcelona, the Spanish Ministry of Science and Innovation (MICINN FIS2008-00114), and Catalunya Caixa for financial support.

References

Bassett DE, Boguski MS, Hieter P (1996) Nature 379:589
Chan J, Fore S, Wachsmann-Hogiu S, Huser T (2008) Lasers Photonics Rev 2:325
Cooper GM (2000) The cell a molecular approach. Sinauer, Sunderland
Delleya PA, Halla MN (1999) J Cell Biol 147:163
Eriksson E, Enger J, Nordlander B, Erjavec N, Ramser K, Goksor M, Hohmann S, Nystrom T, Hanstorp D (2007) Lab Chip 7:71
Eriksson E, Scrimgeour J, Graneli A, Ramser K, Wellander R, Enger J, Hanstorp D, Goksor M (2007) J Opt A Pure Appl Opt 9:S113
Eriksson E, Sott K, Lundqvist F, Sveningsson M, Scrimgeour J, Hanstorp D, Goksor M, Graneli A (2010) Lab Chip 10:617
Gittes F, Schmidt CF (1998) Opt Lett 23:7
Hohmann S, Mager WH (2002) Yeast stress responses. Springer, Berlin
Lakowicz JR (1999) Principles of fluorescence spectroscopy. Springer, Berlin
Lee WM, Reece PJ, Marchington RF, Metzger NK, Dholakia K (2007) Nat Protoc 2:3226
Lee PJ, Helman NC, Lim WA, Hung PJ (2008) BioTechniques 44:91
Petrov DV (2007) J Opt A Pure Appl Opt 9:S139
Rowata AC, Birda JC, Agrestia JJ, Randob OJ, Weitz DA (2009) PNAS 106:18149
Singh GP, Creely CM, Volpe G, Grotsch H, Petrov D (2005) Anal Chem 77:2564
Singh GP, Volpe G, Creely CM, Grotsch H, Geli IM, Petrov DV (2006) J Raman Spectrosc 37:858
Stanbury PF, Whitaker A, Hall SJ (1984) Principles of Fermentation Technology. Pergamon, Oxford
Storey KB, Storey EJM (2002) Cell and molecular response to stress: sensing, signaling and cell adaptation. Elsevier, Amsterdam
Tolic-Norrelykke M, Munteanu EL, Thon G, Oddershede L, Berg-Sorensen K (2004) Phys Rev Lett 93:078102
Tonin M, Bálint S, Mestres P, Martìnez IA, Petrov D (2010) Appl Phys Lett 97:203704
Wadskog I, Forsmark A, Rossi G, Konopka C, Oyen M, Goksor M, Ronne H, Brennwald P, Adler L (2006) Mol Biol Cell 17:4988